3. Y. Hayafuji, T. Shimada, and S. Kawado, in "Semiconductor Silicon 1977," H. R. Duff and E. Sirtl, Editors, p. 750, The Electrochemical Society Softbound Proceedings Series, Princeton, NJ (1977).
4. H. Shiraki, in *ibid.*, p. 546.
5. H. E. Murphy, Proceeding of the SPIE, Vol. 203, pp. 80-87, San Diego, CA (1979).
6. R. L. Rodgers III, p. 196 of Ref. 1.
7. C. H. Sequin, *IEEE Trans. Electron Devices*, **ed-20**, 535 (1973).
8. For tutorial introduction, see H. J. Leamy, L. C. Kimerling, and S. D. Ferris, "Scanning Electron Microscopy," Vol. 1, p. 717, SEM Inc., AMF O'Hare, IL (1978).
9. L. Jastrzebski, P. A. Levine, A. D. Cope, W. F. Kosnocky, W. N. Henry, and D. F. Battson, *IEEE Trans. Electron. Devices*, **ed. 27**, 1694 (1980).
10. For review, see S. M. Hu, *J. Vac. Sci. Technol.*, **14**, 17 (1977).
11. A. W. Fisher and G. L. Schnable, *This Journal*, **123**, 434 (1976).
12. T. Suzuki, A. Mimura, and T. Ogawa, *ibid.*, **124**, 1776 (1977).
13. H. F. Schaake, C. G. Roberts, and A. J. Louis, Advance Research Project Agency Report, Contract No. M00-173-76-C-0280 (1979).
14. G. A. Rozgonyi, *Appl. Phys. Lett.*, **29**, 531 (1976).
15. For measurements of diffusion length done by surface photovoltage, see *e.g.*, Annual Book of ASTM Standards, p. 752, ASTM, Philadelphia (1974).
16. W. F. Kosnocky, J. C. Carnes, M. G. Kovec, P. Levine, F. V. Shallcross, and R. L. Rodgers, *RCA Rev.*, **35**, 2 (1974).
17. L. Jastrzebski and J. Lagowski, Paper 152 presented at The Electrochemical Society Meeting, St. Louis, Missouri, May 11-16, 1980.
18. L. Jastrzebski and P. Zanzucchi, To be published in "Semiconductor Silicon 1981," Minneapolis, MN (May 1981).

Bulk Impurity Charge Trapping in Buried Channel Charge Coupled Devices

M. J. McNutt* and W. E. Meyer

Rockwell International, Anaheim, California 92803

ABSTRACT

Buried channel charge coupled devices are particularly sensitive to the effects of bulk state impurities on such device characteristics as thermal leakage current, charge transfer efficiency, and noise. This paper reviews the statistics relevant to these effects and describes an improved application of the double pulse experiment for probing bulk impurities. This experiment found that the dominant impurity in our devices had an energy level 0.404 eV from one of the bandedges and determined a lower limit of 10^{13} cm^{-3} for the concentration. A close match with previously reported results suggests that this energy level is referenced to the valence band and represents iron. By eliminating the corrosive HCl gas used to getter sodium in the thermal oxides, the source of iron was removed and the affected device characteristics improved about two orders of magnitude.

Bulk impurities, especially in buried channel devices, give rise to several undesirable charge coupled device (CCD) characteristics. Among these are enhanced thermal leakage current, bulk state trapping, and bulk state trapping noise. Thermal leakage current generates charge internally and limits the time during which an empty charge packet can be stored. Bulk state trapping and subsequent emission smears charge into trailing charge packets, thus degrading the signal, and also gives rise to a partition-type bulk state trapping noise. The trapping noise can also dominate as a generation-recombination noise in the output circuit due to the proportionality of this noise power to the square of the bias current.

Mohsen and Tompsett (1) discussed the effects of bulk traps on the performance of buried channel CCD's and described the double pulse technique they used to determine the trap emission time constant. Our purpose in this paper is to review the trapping statistics that include the effects of both energy bands and to describe an efficient implementation of the double pulse measurement technique. We are also interested in identifying the appropriate impurities, and, in our example, we will find a large iron distribution and discuss its source and eventual elimination.

* Electrochemical Society Active Member.
Key words: iron, bulk impurities, charge coupled devices.

Bulk Impurity Statistics

Figure 1 is a band diagram describing the four possible Shockley-Read-Hall (2) trapping transitions assumed to dominate in the device. (*a*) and (*b*) are electron capture and emission rates, and (*c*) and (*d*) are hole capture and emission rates at a trap with energy, E_T. E_C and E_V are the conduction and valence band energies. The relevant statistics can be described by three rate equations

$$dn/dt = (b) - (a) = e_n n_T - c_n n p_T \quad [1]$$

$$dp/dt = (d) - (c) = e_p p_T - c_p p n_T \quad [2]$$

$$dn_T/dt = (a) - (b) - (c) + (d)$$
$$= c_n n p_T - e_n n_T - c_p p n_T + e_p p_T \quad [3]$$

n and p are the electron and hole concentrations, and n_T and p_T are the filled and empty electron bulk state concentrations. c_n and c_p are the electron and hole capture coefficients, and e_n and e_p are the electron and hole emission coefficients.

At equilibrium

$$dn/dt = 0$$
$$n = n_o = N_C \exp[(E_F - E_C)/kT]$$
$$dp/dt = 0$$
$$p = p_o = N_V \exp[(E_V - E_F)/kT] \quad [4]$$

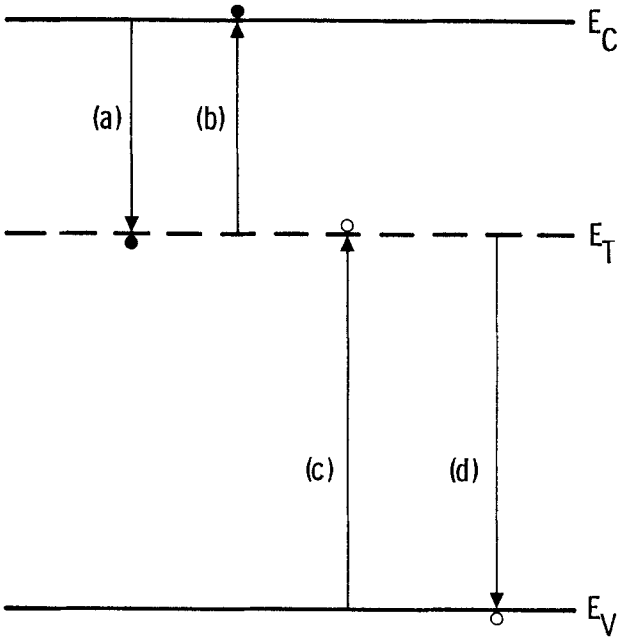

Fig. 1. Energy band diagram indicating bulk state trapping processes.

where N_C and N_V are the effective density of states at the two bandedges and E_F is the Fermi energy. Substituting Eq. [4] into [1] and [2] gives

$$e_n = c_n N_C \exp[(E_T - E_C)/kT]$$
$$e_p = c_p N_V \exp[(E_V - E_T)/kT] \quad [5]$$

To obtain this result we used the Fermi occupation factor in n_T and p_T such that

$$n_T = N_{TT}/(1 + \exp[(E_T - E_F)/kT])$$
$$p_T = N_{TT} \exp[(E_T - E_F)/kT]/(1 + \exp[(E_T - E_F)/kT]) \quad [6]$$

where $N_{TT} = n_T + p_T$ is the total bulk state concentration. Also in equilibrium

$$dn_T/dt = 0$$
$$n_T = N_{TT}(c_n n_o + e_p)/(c_n n_o + e_n + c_p p_o + e_p) \quad [7]$$

where Eq. [3] was substituted along with $p_T = N_{TT} - n_T$.

As noted by Sah (3), Eq. [5] are strictly valid only at thermal equilibrium where they are derived. However, for small deviations from equilibrium we can assume that the electric fields are not large enough to make the capture and emission coefficients field dependent. Also, we will be primarily interested in the temperature dependence of the emission cofficient rather than its absolute value, thus minimizing the effects of nonequilibrium on the measurement accuracy.

In depletion, we have $p = n = 0$, so the emission transitions, (b) and (d), dominate the capture events, (a) and (c), in Eq. [3] giving

$$dn_T/dt \simeq -e_n n_T + e_p p_T$$
$$= -(e_n + e_p) n_T + e_p N_{TT} \quad [8]$$

The solution to Eq. [8] is

$$n_T = \Delta n_T \exp(-t/\tau) + (\tau/\tau_p) N_{TT} \quad [9]$$

where $\tau^{-1} = e_n + e_p$ and $\tau_p^{-1} = e_p$. Let $t = 0$ be the time when the device is switched from equilibrium to depletion so that $n_T(0)$ is given by Eq. [7]. Then from [7] and [9] at $t = 0$ we get

In some cases, [10] can be greatly simplified. For example, in N-type material $n_o >> p_o$, and, if the impurity level is near the middle of the bandgap, $c_n n_o >> e_n$, e_p so that $\Delta n_T \simeq N_{TT} e_n/(e_n + e_p)$. Furthermore, if the energy level is in the upper half of the bandgap, we should have $e_n >> e_p$ and $\Delta n_T \simeq N_{TT}$.

Depending on the location of the impurity energy level, either e_n or e_p normally dominates in τ. For example, if E_T is closer to E_C than E_V, we expect $e_n >> e_p$ from Eq. [5] and so

$$\tau \simeq e_n^{-1} = \{c_n N_C \exp[(E_T - E_C)/kT]\}^{-1} \quad [11]$$

The capture coefficient, c_n, is proportional to $T^{1/2}$ since it contains the thermal velocity factor, and the effective density of states, N_C, is proportional to $T^{3/2}$ (4). Thus, there is a T^2 factor built into the $c_n N_C$ product. This factor can be eliminated by multiplying Eq. [11] by T^2. Then when we take the natural logarithm we get

$$\ln(\tau T^2) = \ln(T^2/c_n N_C) + (E_C - E_T)/kT \quad [12]$$

Now if $\ln(\tau T^2)$ is plotted against $(kT)^{-1}$, the slope of the straight line is $E_C - E_T$ which identifies the impurity energy level. In the other case, if $e_p >> e_n$ (*e.g.*, E_T closer to E_V), then

$$\ln(\tau T^2) = \ln(T^2/c_p N_V) + (E_T - E_V)/kT \quad [13]$$

and the data slope gives $E_T - E_V$.

Trapping occurs when a charge packet in the CCD is transported into a cell that has previously been empty or in depletion. This means that the exponential term in Eq. [9] has at least partially decayed. When the charge packet arrives, electrons fill these empty impurity states almost instantaneously due to the high capture rate caused by the large carrier concentration. However, when the charge packet is transported to the next cell, these electrons stay trapped in the impurity states. We are back to a depletion condition and these electrons are only emitted from the traps according to the exponential time term in Eq. [9]. As the electrons are emitted from the traps they are picked up by trailing charge packets. This total process tends to smear out the CCD signal in time.

The trapping process also gives rise to partition noise in the CCD charge signal due to the constant reapportionment of charge among adjacent cells. Also, there is substantial generation-recombination noise in any currents flowing in the device, particularly in the output circuit where the currents can be substantial. This noise is derived from the constant emission and capture of the current carriers even in a nearly equilibrium condition where the total concentration is constant.

Experimental Procedure

In order to obtain some direct quantitative information on these bulk states, we performed a double pulse charge transfer experiment similar to that of Mohsen and Tompsett (1). This experiment is illustrated in Fig. 2. The device is encased in a controlled temperature environment, and the analog signal charge transfer is driven by a four-phase clock driver. The driver also triggers a double pulse generator at a predetermined interval based on an integral number of clock periods. The double pulse generator puts out two pulses, one immediately following the trigger signal and a second pulse that is delayed from the trigger signal. The delay is manually adjustable, and the width of the two pulses is also adjustable, but the width is normally at least two clock periods. The double pulse output signal from the pulse generator is applied to the shift register input, which samples the signal every clock period and converts voltage to proportional charge. The sampled signal charge is trans-

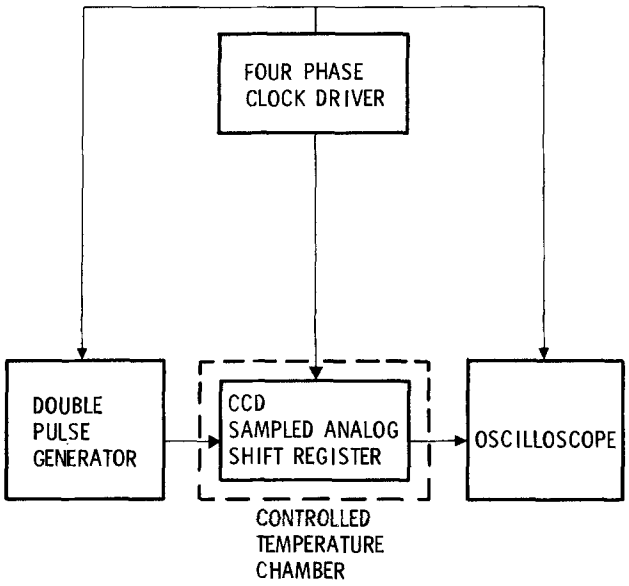

Fig. 2. Block diagram of CCD variable delay double pulse trapping experiment.

it is proportionally converted back to voltage and displayed on the oscilloscope. The oscilloscope uses the same trigger as the pulse generator. Figure 3 contains typical examples of the input and output signals, where, in this case, the output signal has been time shifted to eliminate the shift register delay that would normally occur. As shown in the figure, the pulses applied to the CCD input extend over two clock periods. For each input signal pulse, the resulting output then gives two sample pulses corresponding to the two charge packets that each input signal pulse forms. A more negative output corresponds to a larger charge packet of electrons.

As seen in the output circuit signal, the first charge packet or cell is greatly reduced during transfer down the CCD channel. This is due to trapping of charge by the bulk states. Since most of the traps are filled by the first charge packet, the second charge packet transfers through the CCD with very little loss. There is some loss, however, since the first charge packet is not exposed to all the traps in the channel because of decreases in the charge packet volume due to charge loss.

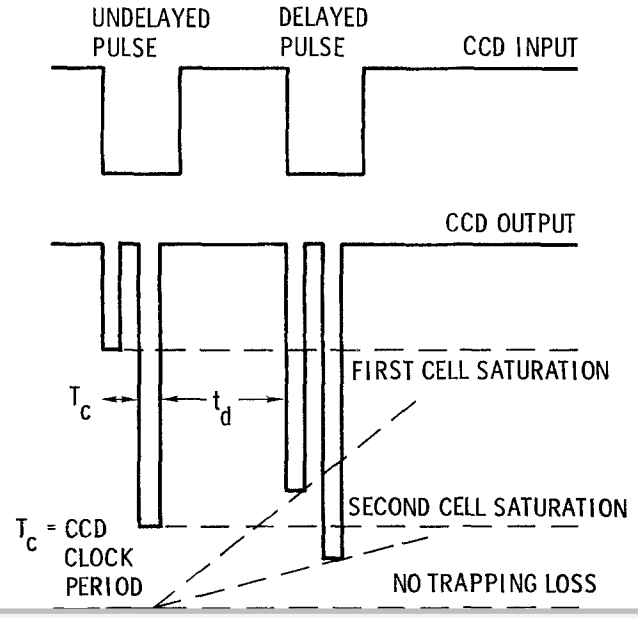

These remaining traps are nearly all filled (in this example) by the second charge packet or the second sample of the first input signal pulse.

In the extreme case of a very large impurity concentration, more than two charge packets may be required to fill the trapping levels. This does not substantially affect the measurement technique as long as a sufficient number of charge packets is provided. This is accomplished by extending the signal pulse width over additional clock periods.

There is a delay, t_d, between the second charge packet from the first input pulse and the first charge packet from the second input pulse as shown in the figure. During this time electrons are emitted from the traps according to the depletion statistics of Eq. [9]. Then when the next charge packet comes along, it fills the recently emptied traps such that its trapping loss is equal to the emission that occurred in the t_d interval. If the emission of trapped charge is large, some of these traps may be missed by the reduced first delayed charge packet. These are then filled by the second delayed charge packet or any additional charge packets that may be required.

If $t_d = 0$, no significant emission from the traps occurs between the charge packet pairs so that no trapping loss occurs in the second pair. At the other extreme, if $t_d >> \tau$, where τ is the trap emission time constant, all the traps empty during t_d and the second charge packet pair experiences the same trapping loss as the first pair. For values of t_d in between these extremes, the second pair trapping loss follows the form

$$Q(t_d) = Q(\infty) + [Q(0) - Q(\infty)] [Q(t_d)/Q(0)] \exp(-t_d/\tau) \quad [14]$$

In Eq. [14], $Q(t_d)$ is the remaining charge at the CCD output in a charge packet delayed by t_d, while $Q(0)$ and $Q(\infty)$ are the remaining charge for charge packets with zero and infinite delays. The quantity $Q(0) - Q(\infty)$ is the charge potentially subject to trapping, and the exponential factor is that of the trap emission rate. As the charge packet moves along the CCD channel losing charge to trapping centers, its volume is reduced and it is exposed to a smaller volume of trapping centers. In a uniform buried channel, this is represented by the factor $Q(t_d)/Q(0)$ where the charge packet volume is assumed proportional to the amount of charge. Finally, we can isolate $Q(t_d)$ in [14] to get

$$Q(t_d) = Q(\infty)/\{1 - [1 - Q(\infty)/Q(0)] \exp(-t_d/\tau)\} \quad [15]$$

Of course the CCD output voltage is proportional to $Q(t_d)$. Thus, by varying t_d and observing the corresponding change in the output voltage, τ can be deduced.

Frequently if the trapping effect is not too large, we have $[1 - Q(\infty)/Q(0)] << 1$, and Eq. [15] can be approximated by

$$Q(t_d) \simeq Q(\infty) \{1 + [1 - Q(\infty)/Q(0)] \exp(-t_d/\tau)\} \quad [16]$$

This approximation becomes more accurate as the exponential factor decays. Since we now have a purely exponential time term in Eq. [16], the time constant, τ, can be determined without regard to the absolute values of $Q(\infty)$ and $Q(0)$. Sometimes the first sample of the delayed signal pulse experiences very large trapping losses such that $Q(\infty) \simeq 0$ and [16] cannot be used. In that case, a second or third sample will have less trapping loss and thus qualify for using Eq. [16]. Since we have to take as many samples of each signal pulse (*i.e.*, stretch the signal pulse over more

Although the time delayed trapping data can be taken in the usual point-by-point manner, a more efficient technique gives a much faster result with an increase in accuracy. This technique uses the fact that the sampling nature of the CCD provides the same size charge packets at the same sample times even as the signal pulse is delayed up to one full clock period. However, when the signal pulse edge passes through the sample aperture time, the charge packet abruptly changes. Thus, when the time delay between pulses is continuously varied, the CCD output photographed by a time exposure clearly indicates the corresponding charge loss variation in the delayed charge packets. Each of the time delayed outputs is displayed for the time it takes to adjust the delay through one CCD clock period. If this time is long enough to expose the film and the delay is varied in a roughly uniform fashion, a good photograph will result. In practice, this typically requires opening the camera shutter for about 5 sec while turning the delay knob on a double pulse generator.

In performing the experiment, it is important to choose a CCD clock period that is much less than τ in order to get many samples of the exponential decay to match with Eq. [15]. Also, the time between the end of the delayed signal pulse and the start of the next signal pulse pair must be long enough to allow all the trapped carriers to be emitted. In other words, the signal pulse pair repetition period must be many τ time constants longer than the longest delay between the two pulses. The first signal pulse then provides the $Q(\infty)$ reference values.

The accuracy of the single photograph method can be better than the technique of recording each time delayed sample separately, even though the individual sample resolution may be less. This is because there is much less opportunity for calibration or temperature drift between t_d readings. Therefore, the relative accuracy between data points is excellent, which is most important in obtaining the time constant, τ, by matching experimental results with Eq. [15]. It should also be noted that this technique of probing bulk impurities by using CCD's is potentially more sensitive than normal capacitance transient methods (5) because the charge packet flows through a number of cells losing trapped charge in each one. In more traditional measurements, only the equivalent of one cell is used. Thus, sensitivity is multiplied by the number of CCD cells. However, to take advantage of this enhanced sensitivity, CCD noise sources such as transfer efficiency noise and output FET noise must be minimized.

Although the double pulse experiment does not by itself give the impurity concentration, N_{TT}, except in the special cases where $N_{TT} \simeq \Delta n_T$, it can give the impurity energy level by finding the slope of Eq. [12] or [13]. This can identify the impurity involved. Since the technique directly measures the adverse CCD characteristic, namely charge transfer trapping loss, it always identifies the impurity that is most injurious to the device, and the measurement can be made near the normal operating temperature.

Experimental Result

An example of the determination of the time constant, τ, at a single temperature is shown in the oscilloscope photo of Fig. 4. This photo is a long time exposure showing the first charge packet pair and a sequence of second charge packet pairs at various delays. The delay time was adjusted continuously from 0 to the edge of the oscilloscope scale while the camera shutter was open. The result is the two exponential decays vividly displayed for the first and second delayed charge packets. The two undelayed charge packet signals are also shown, somewhat bloomed due to the

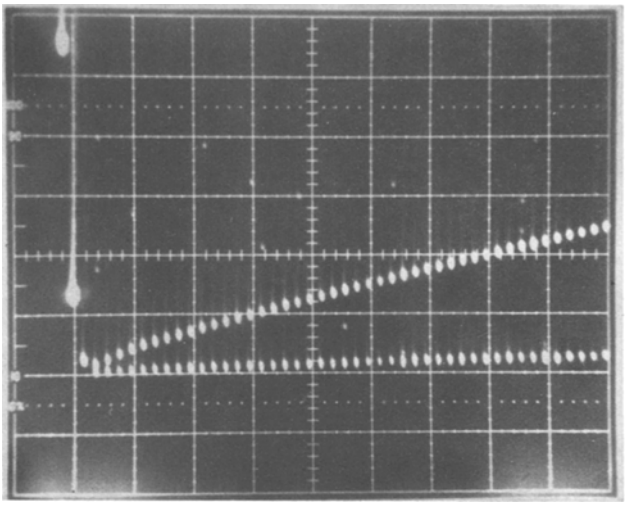

Fig. 4. Long exposure photo of CCD output during variable delay double pulse trapping experiment. Device 30338-1-4-37B; CCD Clock Rate = 50 KHz; Horizontal scale = 100 μsec/div.; Vertical scale = 0.1 V/div.; temperature = 55°F.

erence time. Since the trapping loss is about 25% of the total first charge packet (the zero charge level is well above the top of the scope display), Eq. [16] approximates [15], and a simple exponential decay can be assumed.

For example, let 0V be the top of the vertical scale as an arbitrary reference. The undelayed first charge packet signal is at −0.05V. The delayed first charge packet when the delay is zero (*i.e.*, no charge loss) is at −0.60V, giving a maximum charge loss equivalent to 0.55V. We see a charge loss equivalent to 0.20V at a delay of 700 μsec, so that

$$0.55 - 0.20 = 0.55 \exp(-700 \times 10^{-6}/\tau)$$

$$\tau = 700 \times 10^{-6}/\ln(0.55/0.35)$$

$$= 1550\ \mu\text{sec} \quad \text{at} \quad T = 55°\text{F}$$

Naturally, curve-fitting techniques could be used with Eq. [15] to get more precise values of τ if required. By repeating the experiment at several temperatures, we can plot $\ln(\tau T^2)$ *vs.* $(kT)^{-1}$, and from Eq. [12] and [13], we expect a straight line of slope $E_C - E_T$ or $E_T - E_V$. The experimental results are plotted for a single CCD device in Fig. 5 and they do in fact fall on a least squares fit straight line of slope 0.404 eV $= E_C - E_T$ or $E_T - E_V$. This is an energy level that lies near the midgap of silicon, where we know it can give rise to the most thermal leakage current. The reported energy level closest to this number in silicon is $E_T - E_V = 0.40$ eV for iron (6-8). Iron is known to have one of the highest diffusion coefficients of any impurity in silicon, and its solid solubility is larger than 10^{15} cm^{-3} at our lowest furnace temperatures. An obvious source of iron is the stainless steel plumbing for the gas flow systems and the gas storage tanks. The potentially corrosive HCl gas system used to getter mobile sodium ions from the gate oxides was particularly suspect. By eliminating the HCl gas flow and relying on clean processing and gettering of sodium by our phosphorus-doped polysilicon gates, we obtained an immediate reduction of about two orders of magnitude in thermal leakage and charge trapping in finished devices.

The concentration of trap states from which carriers are emitted after a certain time is given by the first term in Eq. [9], and the concentration of emptied traps after steady state is achieved is represented by

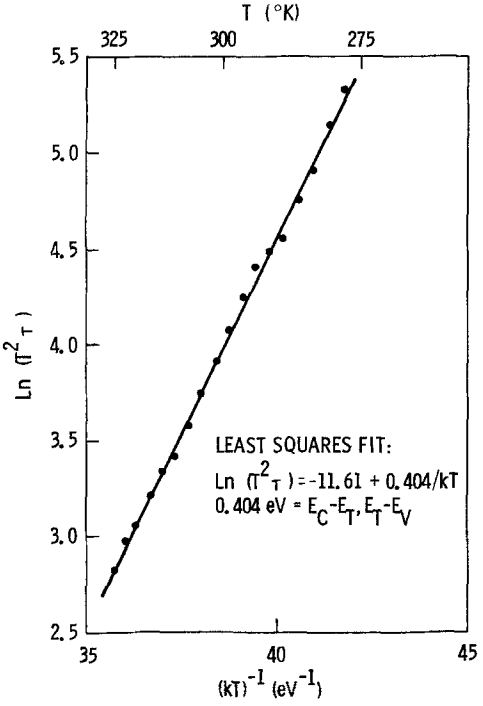

Fig. 5. Experimental data plot yielding bulk state energy level

capture coefficients and the equilibrium doping concentrations.

In our buried N-channel device we have $c_n n_o >> c_p p_o$, and, since the impurity level is near the midgap energy, $c_n n_o >> e_n, e_p$ by comparing Eq. [4] and [5]. Finally, we have assumed that the impurity level emits holes to the valence band so that $e_p >> e_n$. Combining these approximations in Eq. [10], we get $\Delta n_T \simeq (e_n/e_p) N_{TT}$. We have determined $e_p = \tau^{-1}$, but e_n can only be found by another measurement technique. However, we have determined that the concentration of trapped and reemitted carriers, Δn_T, is much less than the impurity concentration or $N_{TT} \simeq (e_p/e_n)\ \Delta n_T >> \Delta n_T$.

Referring to Fig. 4, after the traps have emptied in a full depletion mode so that the first term in Eq. [9] is zero, a full charge packet loses charge represented by a 0.55 drop in output voltage. A second charge packet experiences a 0.13 voltage drop and succeeding full charge packets lose nothing because the traps have reached the equilibrium condition of Eq. [7]. The output circuit has a sensitivity of about 10^{12} V/C, so the 0.55V and 0.13V represent 0.55×10^{-12} C and 0.13×10^{-12} C or a combined total of 4.3×10^6 electrons. These electrons are trapped in a CCD channel that is 250 μm wide $\times$ 1540 μm long $\times$ 1 μm deep for a total volume of 3.8×10^{-7} cm^3. Therefore, the concentration of trapped electrons that can be reemitted is $\Delta n_T = 4.3 \times 10^6/3.8 \times 10^{-7} = 1.1 \times 10^{13}$ cm^{-3}. This represents a lower limit on N_{TT}.

Conclusions

By employing the temperature dependent transfer inefficiency of a CCD, we have been able to identify the impurity causing that inefficiency as iron with an energy level 0.40 eV above the silicon valence band. We have also been able to place a lower limit on the iron concentration of 1.1×10^{13} cm^{-3}. A simplified single photograph variation of the double pulse method greatly facilitated determination of the required emission time constants.

This impurity identification immediately threw suspicion on the furnace plumbing for the HCl gas used to getter the threshold shifting sodium ions in isolation oxides. This plumbing contains iron in the stainless steel tubing and the HCl tanks. By eliminating the HCl gas system, an immediate reduction of about two orders of magnitude in thermal leakage current and in charge trapping was observed in finished devices.

Acknowledgments

We would like to thank R. A. Bredthauer, S. Chung, R. L. Maddox, W. P. Waters, and E. F. Wojtkowski for helpful discussions on the source of iron contamination and its elimination.

Manuscript submitted June 24, 1980; revised manuscript received Nov. 17, 1980.

Any discussion of this paper will appear in a Discussion Section to be published in the December 1981 JOURNAL. All discussions for the December 1981 Discussion Section should be submitted by Aug. 1, 1981.

Publication costs of this article were assisted by Rockwell International.

REFERENCES

1. A. M. Mohsen and M. F. Tompsett, *IEEE Trans. Electron Devices*, **ed-21,** 701 (1974).
2. R. N. Hall, *Phys. Rev.*, **83,** 228 (1951); *ibid.*, **87,** 387 (1952); W. Shockley and W. T. Read, Jr., *ibid.*, **87,** 835 (1952).
3. C. T. Sah, *Proc. IEEE*, **55,** 654 (1967).
4. S. M. Sze, "Physics of Semiconductor Devices," pp. 26-27, John Wiley & Sons, New York (1969).
5. C. T. Sah, L. Forbes, L. L. Rosier, and A. F. Tasch, Jr., *Solid State Electron.*, **13,** 759 (1970).
6. S. M. Sze, "Physics of Semiconductor Devices," pp. 30-32, John Wiley & Sons, New York (1969).
7. A. O. Evwaraye and P. L. Anderson, in "Semiconductor Characterization Techniques," P. A. Barnes and G. A. Rozgonyi, Editors, pp. 61-70, The Electrochemical Society Softbound Proceedings Series, Princeton, N.J. (1978).
8. M. Okuyama, N. Matsunaga, J. W. Chen, and A. G. Milnes, *J. Electron. Mater.*, **8,** 501 (1979).